Chapter 8
Turing and Non-Turing Patterns in Two-Dimensional Prey-Predator Models

Malay Banerjee

Abstract Spatial patterns are ubiquitous in nature, and study of spatio-temporal pattern formation for prey-predator models are initiated based upon the seminal work of Turing on morphogenesis (Turing, Philos Trans R Soc Lond B 237:37–72, 1952). Interactions between individuals of different species over a wide range of spatial and temporal scales often modify the temporal dynamics as well as stability properties of the population distributed over natural landscape. Segel and Jackson (J Theor Biol 37:545–559, 1972) first used reaction-diffusion systems to explain ecological pattern formation by interacting populations. This idea used afterwards to explain pattern formation in plankton systems, semiarid vegetation patterns, invasion by exotic species and distribution of prey-predator distribution over homogeneous space. After the seminal works by Segel and Jackson (J Theor Biol 37:545–559, 1972) and Levin and Segel (Nature 259:659, 1976), researchers were interested to study the Turing-type pattern formation, but now a days it shifted towards non-Turing patterns and spatio-temporal chaos. Empirical evidence in support of spatio-temporal chaotic patterns in interacting populations remain in vein but the resulting patterns have similarity with the irregular distribution over spatial domain. Further, the formation of spatio-temporal chaotic patterns within Turing-Hopf domain remains a controversial issue, whether it arises near the Turing-Hopf boundary or away from it. This article aims to review the recent development of Turing and non-Turing pattern formations in prey-predator models having prey-dependent and ratio-dependent functional response with special emphasis on spatio-temporal chaos.

8.1 Introduction

The spatio-temporal models of predator-prey interaction are studied to understand the role of random mobility of the species, within their habitat, on the stability and persistence of interacting species. Investigation on spatio-temporal models of

M. Banerjee (✉)
Department of Mathematics and Statistics, I.I.T. Kanpur, Kanpur, India
e-mail: malayb@iitk.ac.in

interacting population reveal that the movement of the individuals of one or more species some time act as a stabilizing factor and in some cases they are capable to induce some destabilization. Interestingly, destabilization of homogeneous distribution of population is not a threat towards the survival of population rather it may settle down to inhomogeneous distribution of individuals over their habitats producing localized patches. These localized patches may be time invariant or may not be. Diffusivity of individuals has power to stabilize as well as destabilize the coexistence scenario. As a result, researchers are interested to study various types of stationary and non-stationary spatio-temporal pattern formation by the interacting populations. Mathematical analysis and numerical simulation of spatio-temporal models provide the idea that how individuals of certain species are distributed over two dimensional landscapes or within the aquatic environment. In reality, the distribution of plant and animal populations is not homogeneous rather they are packed in localized patches. These localized patches either remain fixed or change with time [21]. Time invariant patches and the patches moving with time correspond to stationary and non-stationary patterns. Non-stationary patterns may be oscillatory, quasi-periodic or chaotic. Various types of resulting patterns can be classified as spot pattern, labyrinthine pattern, stripe pattern, target pattern, spiral pattern, tip-splitting pattern and interacting spiral pattern [7, 18].

Significance and importance of spatial aspect towards the stabilization and long term existence of certain species was first observed by Gause [24]. His observation was based upon the laboratory experiments to study growth of *paramecium* and *didinum* [9]. Effect of spatial distribution on stability of population and persistence or extinction properties was studied by Luckinbill [39, 40]. A detailed discussion on the role of space and mobility of individuals on the interaction of ecological species are available in the book by Okubo and Levin [48]. All the research works on spatio-temporal pattern formation due to small perturbation to the homogeneous distribution of population are based upon the seminal work of Turing [63]. Turing's idea of pattern formation in reaction-diffusion system was first applied to justify ecological pattern formation by Segel and Jackson [57]. The same idea was carried out to explain to explain patchy distribution in plankton community by Levin and Segel [37] and for semiarid vegetation patterns by Klausmeier [32]. Now a days the literature on pattern formation by interacting populations is very rich as huge number of articles is published in this direction and a wide variety of spatial patterns are reported [2, 8, 9, 11, 12, 15, 16, 21, 23, 30, 32, 41, 44–46, 51–53, 58, 59, 66]. Initially the works in this direction was focused on the Turing patterns only. Recently, attempts are made to study the non-Turing patterns with special emphasis on spatio-temporal chaos. Few recent works demonstrated the mechanism of spatio-temporal chaotic patterns which are biologically realistic to some extent. But empirical evidence and field data supporting spatio-temporal chaos are not abundant. Rather, existence of chaos in ecological system still remains a controversial issue. However, spatio-temporal chaotic patterns are able to explain the irregular distribution of population which is frequently observed in nature.

Majority of literature on spatio-temporal pattern formation in the spatially extended prey-predator models are focused with the models having prey-dependent

functional response and death rate of the predators is directly proportional to their density [23, 41, 51]. These types of models are unable to produce Turing patterns. But the consideration of prey-predator models with nonlinear death rate for predator are capable to exhibit Turing patterns [12, 44, 64]. But Turing and non-Turing pattern formation in case of spatially distributed populations with ratio-dependent functional response are now getting attention from the researchers [2, 6, 8, 9, 68]. As the temporal models of prey-predator interaction with ratio-dependent functional response produce much richer dynamics (see [5, 29, 31, 34, 35, 70] and references cited therein) compared to the models with prey-dependent functional response so it is expected that the spatial extension of ratio-dependent prey-predator model will produce a wide variety of patterns. Initially the ratio-dependent functional response faced strong criticism as it is undefined at the origin [1, 3, 4, 25]. Arditi and Ginzburg [4] argued that the functional response could be a function of the prey-to-predator ratio when interaction is characterized by the heterogeneity of space and time. Further, the dependence of the functional responses upon the densities of prey and predators are now established by the theoretical biologists. The ratio-dependent functional response is more suitable when predators have to search for prey individuals and hence they have to compete among themselves.

Formation of spatio-temporal patterns are obtained by analyzing the partial differential equation models of prey-predator interaction. Most of the models are extension of ordinary differential equation models by incorporating diffusion terms to model the mobility of the individuals of each species. Classical Gause type prey-predator system is governed by the system of coupled ordinary differential equations

$$\frac{dN}{dT} = Q(N, K)N - R(N, P)P,$$
$$\frac{dP}{dT} = eR(N, P)P - M(P)P, \tag{8.1}$$

subjected to non-negative initial conditions [22]. In above formulation, $N \equiv N(T)$ and $P \equiv P(T)$ denote the prey and predator population densities respectively at any instant of time 'T'. $Q(N, K)$ is the density-dependent per capita growth rate of prey in absence of predator and the positive constant K stands for the environmental carrying capacity for the prey. $Q(N, K)$ satisfies some basic properties: $Q(K, K) = 0$, $Q(0, K) > 0$, $\lim_{K \to \infty} Q(0, K) < \infty$, $Q_N(N, K) < 0$, $Q_K(N, K) \geq 0$, $\lim_{K \to \infty} Q_N(N, K) = 0$ and $Q_{NK}(N, K) > 0$. The sole link between the growth of prey and predator populations is the functional response $R(N, P)$, which is a function of both the prey and predator population and stands for the amount of prey biomass consumed by per predator per unit of time. Further, it is assumed for a wide range of prey-predator models that the growth rate of the predators due to prey consumption is simply proportional to the functional response. The proportionality constant is e ($0 < e < 1$) and is known as the conversion efficiency. Several authors have considered the fact that the consumption of prey biomass by their predators is solely depend upon the abundance of prey biomass only and hence

the functional response is a function of prey population only, $Q(N, P) \equiv Q(N)$. This type of functional response in known as prey-dependent functional response. $Q(N)$ always satisfies two properties, $Q(N) > 0$ for all $N > 0$ and $Q(0) = 0$ and monotonic prey-dependent functional response satisfies additional condition $Q_N(N) > 0$ [19]. There are some non-monotonic functional responses, namely Holling type-IV [33] and Monod-Haldane type functional response [10, 26, 49]. The ratio-dependent functional response can be obtained from the prey dependent functional response, replacing N by N/P. The ratio-dependent functional response, given by $Q(N/P)$, satisfy additional condition $\lim_{(N,P)\to(0,0)} PQ(N/P) = 0$ [34]. There are several evidences like field data, laboratory experiments etc. towards the consideration of functional response as a function of both the prey and the predator population densities. Beddington-DeAngelis functional response [62], ratio-dependent functional response [3, 4] are examples of the functional response involving predator population density also. $M(P)$ is the per capita intrinsic death rate for the predator and mostly it is assumed to be a constant. The Gause type prey-predator model is capable to describe the dynamic behavior of specialist predator's only as the growth rate of predator population is zero in the absence of the prey [13].

Here we first recall the mathematical criteria for the Turing pattern formation for spatio-temporal prey-predator model where individuals are assumed to be distributed over two-dimensional bounded domain. Mathematical model is described in terms of non-homogeneous parabolic partial differential equations subjected to positive initial conditions and no-flux boundary conditions. Then we look at the pattern formation for the models having ratio-dependent functional response terms. The spatial extension of classical Holling-Tanner model is revisited to show the transition in pattern formation and sensitivity of patterns to initial conditions. Most of the results discussed here are already available in literature [8, 9, 65]. Results are recollected here to ensemble the varieties of patterns produced by the interacting prey-predator models whose temporal counterpart exhibit very rich dynamics. The role of temporal instability and spatial instability to induce spatio-temporal chaotic pattern is discussed in the concluding section.

8.2 Basic Spatio-Temporal Model

A general spatio-temporal prey-predator model is governed by the following system of two nonlinear coupled partial differential equations

$$\frac{\partial N(T, X, Y)}{\partial T} = NF(N, P) + D_N \left(\frac{\partial^2 N}{\partial X^2} + \frac{\partial^2 N}{\partial Y^2} \right)$$

$$\frac{\partial P(T, X, Y)}{\partial T} = PG(N, P) + D_P \left(\frac{\partial^2 P}{\partial X^2} + \frac{\partial^2 P}{\partial Y^2} \right) \tag{8.2}$$

subjected to known non-negative initial distribution of populations,

$$N(0, X, Y) = N_0(X, Y) \geq 0, \; P(0, X, Y) = P_0(X, Y), \; (X, Y) \in \Gamma, \quad (8.3)$$

and zero-flux boundary conditions

$$\frac{\partial N}{\partial \nu} = \frac{\partial P}{\partial \nu} = 0, \; (T, X, Y) \in (0, \infty) \times \partial \Gamma. \tag{8.4}$$

$N \equiv N(T, X, Y)$ and $P \equiv P(T, X, Y)$ denote the density of the prey and the predators respectively at any instant of time 'T' and at the position (X, Y) within the square bounded domain Γ having boundary $\partial \Gamma$. $F(N, P)$ and $G(N, P)$ are the per capita growth rates of the prey and predator population respectively and D_N, D_P are their rate of diffusions. The governing system (8.2) can be written in terms of dimensionless variables as follows [47]

$$\frac{\partial n(t, x, y)}{\partial t} = nf(n, p) + \left(\frac{\partial^2 n}{\partial x^2} + \frac{\partial^2 n}{\partial y^2} \right)$$

$$\frac{\partial p(t, x, y)}{\partial t} = pg(n, p) + d \left(\frac{\partial^2 p}{\partial x^2} + \frac{\partial^2 p}{\partial y^2} \right) \tag{8.5}$$

subjected to the initial conditions,

$$n(0, x, y) = n_0(x, y) \geq 0, \; p(0, x, y) = p_0(x, y), \; (x, y) \in \Omega, \quad (8.6)$$

and boundary conditions

$$\frac{\partial n}{\partial \nu} = \frac{\partial p}{\partial \nu} = 0, \; (t, x, y) \in (0, \infty) \times \partial \Omega. \tag{8.7}$$

Here n, p are dimensionless population densities, t, x, y are dimensionless independent variables and $d \; (= D_P/D_N)$ is the ratio of diffusivities. Majority of the research works are based upon the dimensionless versions of the nonlinear coupled partial differential equations as they contain less number of parameters. The temporal model corresponding to the spatio-temporal model (8.5) is a system of two nonlinear coupled ordinary differential equations

$$\frac{dn(t)}{dt} = nf(n, p),$$

$$\frac{dp(t)}{dt} = pg(n, p), \tag{8.8}$$

with non-negative initial conditions $n(0)$, $p(0) \geq 0$. This type of system admits a trivial equilibrium point $(0, 0)$ (provided $f(.)$ and $g(.)$ are defined at $(0, 0)$), one or two axial equilibrium points and coexisting equilibrium point(s) is(are) solution(s)

of the system of algebraic equations $f(n, p) = 0 = g(n, p)$ [22, 33]. The number of axial and interior equilibrium point solely depends upon the functional forms of $f(n, p)$ and $g(n, p)$. Let $E_*(n_*, p_*)$ denotes interior equilibrium point and for Turing-instability conditions we need the local asymptotic stability condition of E_* only. The Jacobian matrix for the system (8.8) evaluated at E_* is given by

$$J_* \equiv J(n, p)|_{E_*} = \begin{bmatrix} j_{11} & j_{12} \\ j_{21} & j_{22} \end{bmatrix}, \qquad (8.9)$$

where

$$j_{11} = n \frac{\partial f}{\partial n}\Big|_{E_*}, \quad j_{12} = n \frac{\partial f}{\partial p}\Big|_{E_*}, \quad j_{21} = p \frac{\partial g}{\partial n}\Big|_{E_*}, \quad j_{22} = p \frac{\partial g}{\partial p}\Big|_{E_*}.$$

Interior equilibrium point E_* is locally asymptotically stable whenever the following conditions are satisfied,

$$\text{Tr}(J_*) = j_{11} + j_{12} < 0, \qquad (8.10)$$

$$\text{Det}(J_*) = j_{11} j_{22} - j_{12} j_{21} > 0. \qquad (8.11)$$

According to the Routh–Hurwitz criteria [47], $\text{Tr}(J_*) < 0$ and $\text{Tr}(J_*) > 0$ ensure that the two eigenvalues of J_* are negative or having negative real parts. The interior equilibrium point looses stability through Hopf-bifurcation [28] when $\text{Tr}(J_*) = 0$. Solving the equation $\text{Tr}(J_*) = 0$ in terms any parameter 'α' (say) involved with the system we can find the Hopf-bifurcation threshold (denoted by α_H, for convenience) and instability of interior equilibrium point is ensured when the transversality condition for the Hopf-bifurcation is satisfied. This transversality condition is $\frac{d}{d\alpha} \text{Tr}(J_*)\Big|_{\alpha=\alpha_H} \neq 0$. Small amplitude periodic solution arises through Hopf-bifurcation and interior equilibrium point is surrounded by a limit-cycle. The stability or instability of the limit-cycle is determined through the sign of first Lyapunov number [36, 50].

The components of interior equilibrium point define a homogeneous steady-state for the reaction-diffusion system. $n(t, x, y) = n_*$ and $p(t, x, y) = p_*$ satisfy the system of partial differential equations (8.5) along with the initial and boundary conditions. The condition under which a small heterogeneous perturbation around the homogeneous steady-state develop with the advancement of time is known as the Turing instability condition. The development of small inhomogeneous perturbation leads to spatio-temporal pattern formation.

To obtain the Turing instability condition, the perturbation around the homogeneous steady-state is defined by

$$n(t, x, y) = n_* + u(t, x, y), \ p(t, x, y) = p_* + v(t, x, y), \qquad (8.12)$$

where $u = \epsilon_1 e^{\lambda t} \cos(k_x x) \cos(k_y y)$ and $v = \epsilon_2 e^{\lambda t} \cos(k_x x) \cos(k_y y)$. ϵ_1 and ϵ_2 are two small non-zero real numbers and $k = \sqrt{k_x^2 + k_y^2}$ is the wave number. Substituting (8.12) into (8.5) and then linearizing the system about (n_*, p_*) we get the following characteristic equation

$$|J_k - \lambda I_2| = 0, \tag{8.13}$$

where

$$J_k = J_* - k^2 \text{diag}(1, d) \, I_2 = \begin{bmatrix} j_{11} - k^2 & j_{12} \\ j_{21} & j_{22} - dk^2 \end{bmatrix}. \tag{8.14}$$

For Turing instability requires that at least one eigenvalue of the matrix J_k must have positive real root. Violation of at least one of the following two inequalities imply the onset of Turing instability,

$$j_{11} + j_{12} - (1 + d)k^2 < 0, \tag{8.15}$$

$$h(k^2) \equiv d(k^2)^2 - (dj_{11} + j_{22})k^2 + j_{12}j_{21} - j_{12}j_{21} > 0. \tag{8.16}$$

The condition (8.15) is always satisfied when interior equilibrium point of the temporal model is locally asymptotically stable and d, $k^2 > 0$. The only relevant instability condition can be achieved through the violation of the inequality (8.16) for a range of values of k. $h(k^2)$ attains its minimum at $k^2 = k_T^2$, where

$$k_T^2 = \frac{dj_{11} + j_{22}}{2d} > 0. \tag{8.17}$$

As $j_{11} + j_{22} < 0$ and k_T is a real quantity, the feasible existence of k_T demands that j_{11} and j_{22} must be of opposite sign. The models for which $j_{11} j_{22} \geq 0$, one can not find any Turing pattern. As 'd' is a positive parameter, the conditions $j_{11} + j_{22} < 0$ and $\frac{dj_{11} + j_{22}}{2d} > 0$ are satisfied simultaneously whenever j_{11} and j_{22} are of opposite sign, that is, $j_{11} j_{22} < 0$. Substituting $k = k_T$ in the expression of $h(k^2)$, we find a sufficient condition for Turing instability,

$$0 < 2\sqrt{d}\,\sqrt{j_{12}j_{21} - j_{12}j_{21}} < dj_{11} + j_{22}. \tag{8.18}$$

Turing bifurcation curve is given by $h(k_T^2) = 0$ which defines a boundary in the parametric space. Turing instability cannot occur in the case of equal diffusivity (i.e. $d = 1$). For prey-predator models, in general, $j_{22} \leq 0$ and again one can not find the situation of Turing instability whenever $j_{22} = 0$. For $j_{22} < 0$, the occurrence of Turing instability demands the satisfaction of the restriction $d > -\frac{j_{22}}{j_{11}} > 1$.

Now $h(k^2)$ is a continuous function of k^2, which is a parabola, and for Turing instability we need $h(k_T^2) < 0$. In this case we find two values of k^2 (by solving (8.16) for k^2) which are given by

$$k_{1,2}^2 = \frac{dj_{11} + j_{22} \mp \sqrt{(dj_{11} + j_{22})^2 - 4d(j_{11}j_{22} - j_{12}j_{21})}}{2d}, \qquad (8.19)$$

such that $h(k^2) < 0$ whenever $k^2 \in (k_1^2, k_2^2)$. This interval gives us range of unstable wave numbers.

8.3   Turing and Non-Turing Patterns

In this section we explore the structure of Turing bifurcation domains and various types of stationary and non-stationary patterns exhibited by two dimensional prey predator models with ratio dependent and prey dependent functional responses. The classical Gauss type prey-predator models with prey dependent function response fail to produce any Turing patterns. Temporal dynamics of those models are governed by the system of nonlinear coupled ordinary differential equations

$$\frac{dn}{dt} = nq(n) - r(n)p,$$

$$\frac{dp}{dt} = er(n)p - mp, \qquad (8.20)$$

subjected to positive initial conditions. $q(n)$ is per capita growth rate of prey in the absence of predators, $r(n)$ denotes the rate of grazing by the predators, e $(0 < e < 1)$ is the conversion efficiency and 'm' is the intrinsic death rate for predators. Spatio-temporal models with these type of temporal counterpart are unable to produce Turing patterns as $j_{22} = 0$ and hence the condition $j_{11}j_{22} < 0$ can not be satisfied.

In the forthcoming subsections, we are going to discuss three different models for prey-predator interactions which exhibit Turing as well as non-Turing patterns for specific choices of parameter values. Two ratio-dependent prey-predator models and Holling-Tanner model with prey-dependent functional response is considered here as all of them exhibit Turing patterns. To obtain the spatio-temporal patterns, numerical simulations are performed using the Euler scheme for the reaction part and five point explicit finite difference scheme for the diffusion part. All the numerical simulation results presented here are obtained by considering zero-flux boundary conditions and small amplitude random perturbation around homogeneous steady-state (if not specified otherwise) [42]. The choices of the lattice size along with temporal and spatial stepping are mentioned at relevant places. The domain of integration, for all the simulation results presented here, are taken as square domain.

8.3.1 Ratio-Dependent Prey-Predator Model

Dynamical interaction between prey and predator species with ratio-dependent functional response is governed by the following system

$$\frac{\partial n(t, x, y)}{\partial t} = n(1 - n) - \frac{\alpha n p}{n + p} + \left(\frac{\partial^2 n}{\partial x^2} + \frac{\partial^2 n}{\partial y^2} \right),$$

$$\frac{\partial p(t, x, y)}{\partial t} = \frac{\beta n p}{n + p} - \gamma p + d \left(\frac{\partial^2 p}{\partial x^2} + \frac{\partial^2 p}{\partial y^2} \right), \tag{8.21}$$

subjected to the initial and boundary conditions as described in the previous section. The parameters α, β, γ and d are dimensionless positive parameters and detailed description of the model can be found in [9]. In [9], we have obtained spatio-temporal patterns within and outside the Turing domain for specific choices of parameter values.

The temporal dynamics of the system (8.21) is governed by the following system of equations

$$\frac{dn(t)}{dt} = n(1 - n) - \frac{\alpha n p}{n + p},$$

$$\frac{dp(t)}{dt} = \frac{\beta n p}{n + p} - \gamma p, \tag{8.22}$$

with the initial condition $n(0) n_0 \geq 0$ and $p(0) p_0 \geq 0$. The function $\frac{np}{n + p}$ is not defined at the origin but $\lim\limits_{(n, p) \to (0, 0)} \left[n(1 - n) - \frac{\alpha n p}{n + p} \right] = 0$ and $\lim\limits_{(n, p) \to (0, 0)} \left[\frac{\beta n p}{n + p} - \gamma p \right] = 0$. To maintain the continuity of the system in $\mathbf{R}_{0+}^2 = \{(n, p) \in \mathbf{R}^2 : n, p \geq 0\}$, we can redefine [9] the temporal model as follows

$$\frac{dn(t)}{dt} = n(1 - n) - \frac{\alpha n p}{n + p}, \quad \frac{dp(t)}{dt} = \frac{\beta n p}{n + p} - \gamma p, \ (n, p) \neq (0, 0),$$

$$\frac{dn(t)}{dt} = \frac{dp(t)}{dt} = 0, \ (n, p) = (0, 0). \tag{8.23}$$

In a similar fashion the spatio-temporal model (8.21) can be redefined easily. The temporal steady-states for the system (8.23) are $(0, 0)$ (trivial equilibrium), $(1, 0)$ (axial equilibrium) and unique interior equilibrium point $(n_*, p_*) = \left(1 - \frac{\alpha(\beta - \gamma)}{\beta}, \frac{(\beta - \gamma)n_*}{\gamma} \right)$. The feasibility conditions for the existence of

interior equilibrium point are given by $\alpha < \dfrac{\beta}{\beta - \gamma}$ and $\gamma < \beta$. These two conditions are automatically satisfied for $\alpha < 1$.

Nature and stability properties of various equilibrium points are available in [9, 17, 35, 70] and references cited therein. Local asymptotic stability condition of E_* is given by

$$\alpha < \alpha_* \equiv \frac{\beta}{\beta + \gamma} \left(\gamma + \frac{\beta}{\beta - \gamma} \right). \tag{8.24}$$

The stability condition is automatically satisfied for $\alpha \leq 1$ and in fact, E_* is a global attractor. For $\alpha > 1$, interior equilibrium point losses stability when α crosses the threshold magnitude α_* and limit-cycle arises through Hopf-bifurcation. Limit cycle encircling the interior equilibrium point is stable and unique [5].

We now discuss the spatio-temporal pattern formation by the model (8.21). To obtain the Turing patterns, we have to identify the parameter values which satisfy the conditions (8.10), (8.11) and (8.18). $u(t, x, y) = u_*$ and $v(t, x, y) = v_*$ define a homogeneous steady-state for the system (8.21). Diffusive instability never sets in for $\alpha \leq 1$ as $j_{11} = (\alpha - 1) - \dfrac{\alpha \delta^2}{\beta^2} \leq 0$ and $j_{22} = -\dfrac{(\beta - \delta)\delta}{\beta} < 0$ ($\beta > \delta$ whenever E_* is feasible). Note that the ratio of diffusivities is always positive and hence the condition (8.17) can not be satisfied for $\alpha \leq 1$. We find Turing patterns for the model (8.21) only for $\alpha > 1$ and suitable choice of the parameter 'd'.

Our next task is to determine the Turing bifurcation domain and obtain Turing and non-Turing patterns for the model (8.21). The parameters β and γ are fixed at the values $\beta = 1$ and $\gamma = 0.6$ (hypothetical parameter set [9]) and consider α and d as bifurcation parameters. For chosen parameter set, the Turing bifurcation curve and Hopf-bifurcation curves are shown in Fig. 8.1. These two bifurcation curves divide the domain into four parts and we obtain stationary as well as non-stationary
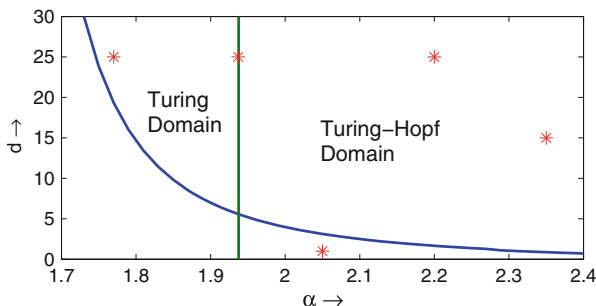

Fig. 8.1 Bifurcation diagram is obtained for $\beta = 1$ and $\gamma = 0.6$, *blue curve* is the Turing-bifurcation curve and the *vertical green line* is Hopf-bifurcation curve. *Red asterisks* represent the points in the $\alpha - d$-parametric space corresponding to which the numerical simulations for the model (8.23) are performed
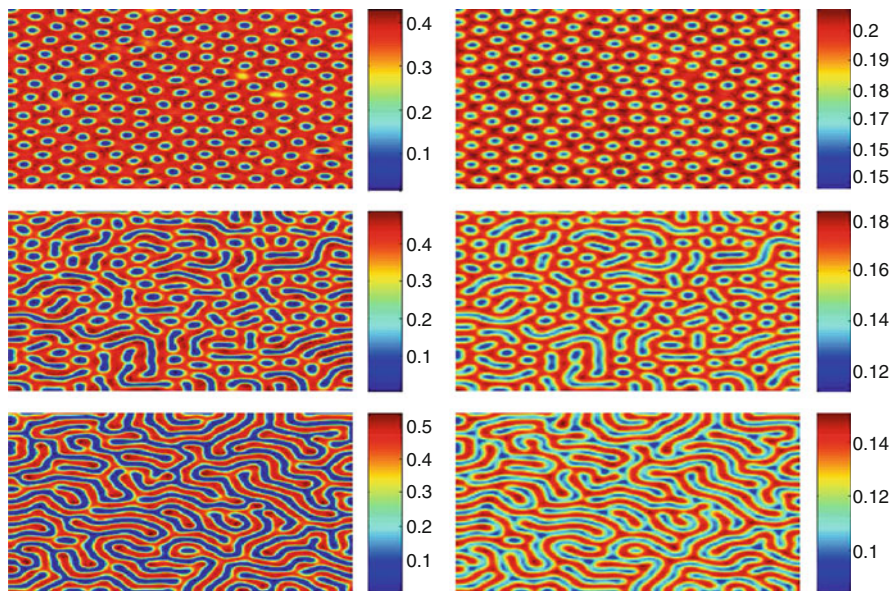
Fig. 8.2 Patterns exhibited by prey (*left column*) and predator (*right column*) for $(\alpha, d) = (1.77, 25)$ (*upper panel*); $(\alpha, d) = (1.9375, 25)$ (*middle panel*); $(\alpha, d) = (2.2, 25)$ (*lower panel*). All the patterns presented here are stationary patterns and obtained at $t = 700$

spatio-temporal patterns for parameter values taken from the Turing domain and Turing Hopf-domain respectively.

We fix the ratio of diffusivity at $d = 15$ and take three different values of α, namely $\alpha = 1.77, 1.9375, 2.2$ and correspondingly the three points lying in the Turing domain, on the Hopf-bifurcation curve and in the Turing-Hopf domain respectively of the parameter space (see Fig. 8.1). For these choices of parameter values, the model (8.21) is simulated over a 400×400 lattices and taking $\Delta t = 0.01$ and $\Delta x = \Delta y = 1$. To ensure that the reported patterns are free from numerical artifacts, the same model is simulated with smaller step sizes and the simulation results remain invariant. Resulting patterns are presented in Fig. 8.2, the reported patterns are observed at $t = 700$. For $(\alpha, d) = (1.77, 25)$ we find cold-spot pattern, these cold spots started coalescing at $(\alpha, d) = (1.9375, 25)$ and ultimately leads to labyrinthine pattern when $(\alpha, d) = (2.2, 25)$. All these patterns are stationary patterns as they remain unaltered with the further increase in time. This stationary property is illustrated in Fig. 8.3, where spatial average of population densities are plotted against time. The labyrinthine pattern sustain for $d = 25$ whenever $\alpha < 2.5$. There is no feasible homogeneous steady-state for $\alpha \geq 2.5$. It is important to note here that the temporal steady-state is unstable and started oscillating for $\alpha > 1.9375$ (the Hopf-bifurcation threshold for $\beta = 1$ and $\delta = 0.6$) but stationary distribution for both the species are obtained here. One natural question arises here, whether we always get stationary patterns for all
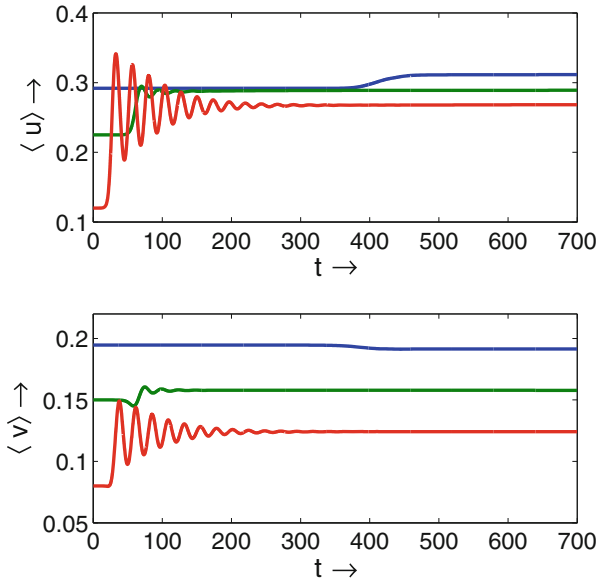
Fig. 8.3 Plot of spatial averages for prey and predator population for $\alpha = 1.77$ (*blue curve*); $\alpha = 1.9375$ (*green curve*); $\alpha = 2.2$ (*red curve*) and $d = 25$

parameter values within the Turing-Hopf domain where the system loses its stability behavior under small amount temporal and spatial perturbation to the homogeneous steady-state. To answer this question we have to examine the patterns for other choices of parameter sets within the Turing-Hopf domain.

There is no mechanism by which one can choose the parameter values within the Turing-Hopf domain for which we find non-stationary patterns. To illustrate such pattern, we choose $\alpha = 2.35$ and $d = 15$. Numerical simulations with this choice of parameter values reveal spatio-temporal chaos and resulting patterns never settle down to any stationary inhomogeneous distribution. Rather they continue to develop irregular patterns which can be classified as spatio-temporal chaotic pattern. In Fig. 8.4 the spatial distribution of prey and predator species is presented at $t = 1,500$ along with the spatial average of the two species against time. Phase portrait for the population density of prey verses predator at the location (200, 200) is also plotted in the same figure. The illustrations at the lower panel clearly indicates the chaotic nature of population distributions.

The spatio-temporal patterns we discussed so far for the model (8.21) are obtained for the choice of parameter values inside the Turing domain. Now we can see that the inhomogeneous spatial distribution of prey and predator species can be obtained for the choice of parameter values outside the Turing domain. For this purpose, we choose $\alpha = 2.05$ and $d = 1$. Numerical simulation reveals that the resulting pattern is chaotic. From the sake of brevity the spatio-temporal chaotic nature is not illustrated here. This chaotic nature can be verified in a similar manner as explained in the last paragraph. In Fig. 8.5, the spatial distributions of prey species
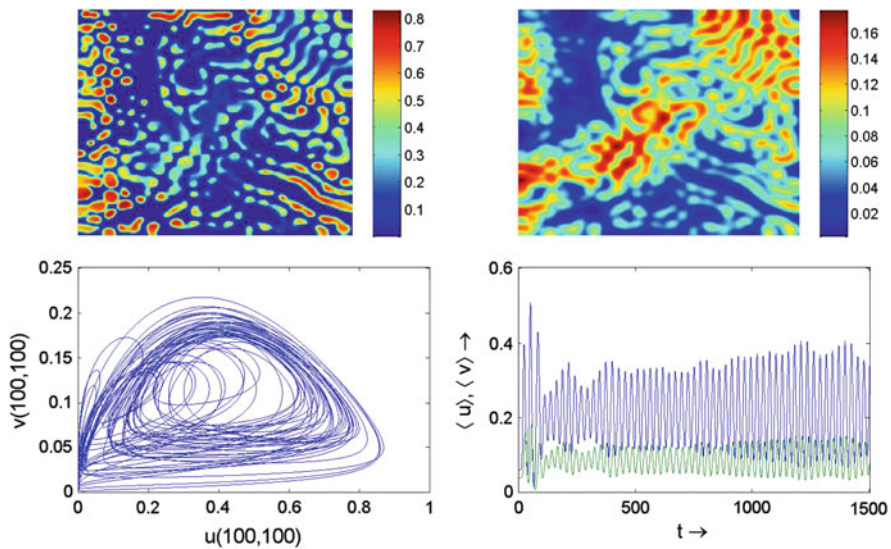
Fig. 8.4 *Upper panel*: Spatial distribution of prey (*left*) and predator (*right*) at $t = 1,500$ for $\alpha = 2.35$ and $d = 15$. *Lower panel*: Plot of $u(200, 200)$ against $v(200, 200)$ (*left*) and time evolution of spatial averages of prey and predator density (*right*)
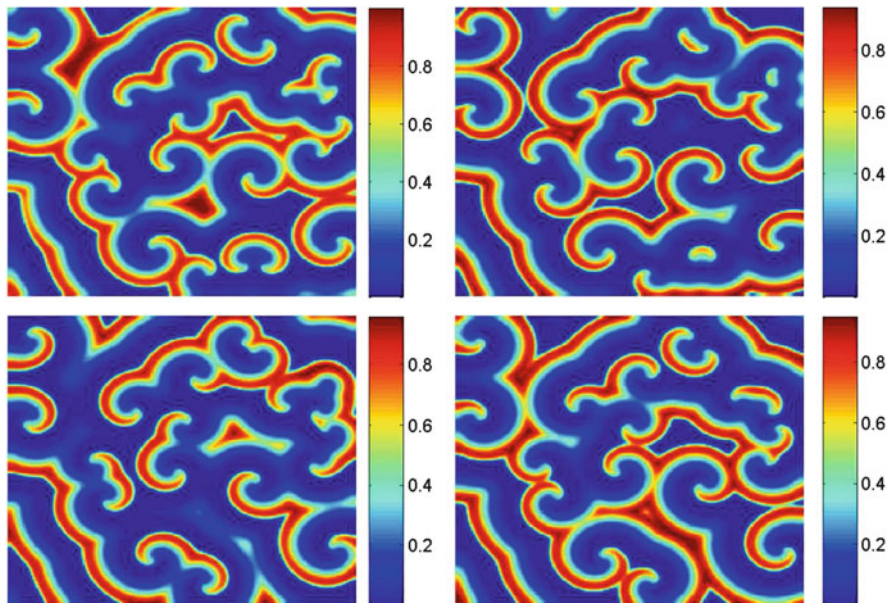

Fig. 8.5 Spatio-temporal chaotic pattern is observed for $\alpha = 2.05$ and $d = 1$. Spatial distribution for prey population at $t = 500$ (*upper-left*); $t = 600$ (*upper-right*); $t = 700$ (*lower-left*) and $t = 800$ (*lower-right*). It is a dynamic pattern

at different time is presented to show the continuous change in the distribution of species. Patterns are presented here for the latest time $t = 800$, but the existence of similar patterns are verified with long time simulations. This type of pattern is classified as interacting spiral pattern and it is a non-Turing pattern.

8.3.2 Ratio-Dependent Holling-Tanner Model

Classical Holling-Tanner type prey-predator was developed to describe the interaction between generalist predator and their most favorable food as prey. Holling-Tanner type prey-predator model with ratio-dependent functional response was proposed and analyzed by Liang and Pan [38]. Recently, we have studied the stationary and non-stationary pattern formation for the spatio-temporal Holling-Tanner model with ratio-dependent functional response [8]. Spatio-temporal dynamics of the Holling-Tanner type prey-predator model with ratio-dependent functional response is governed by the following system of nonlinear coupled parabolic partial differential equations

$$\frac{\partial n(t, x, y)}{\partial t} = n(1 - n) - \frac{np}{n + \delta p} + \left(\frac{\partial^2 n}{\partial x^2} + \frac{\partial^2 n}{\partial y^2} \right),$$

$$\frac{\partial p(t, x, y)}{\partial t} = \xi \left(\eta - \frac{p}{n} \right) p + d \left(\frac{\partial^2 p}{\partial x^2} + \frac{\partial^2 p}{\partial y^2} \right), \tag{8.25}$$

subjected to known positive initial conditions $n_0(x, y)$, $p_0(x, y) \geq 0$, $(x, y) \in \Gamma$ and zero-flux boundary conditions $\frac{\partial n}{\partial \nu} = \frac{\partial p}{\partial \nu} = 0$ for $(t, x, y) \in (0, \infty) \times \partial \Gamma$. This model is also undefined at the origin and the reaction kinetics at the origin can be defined in a similar fashion as described in the previous subsection. The non-zero homogeneous steady-state is $(n_*, p_*) = \left(1 - \frac{\eta}{\eta \delta + 1}, \eta n_* \right)$ and the feasibility condition is $\eta < \eta \delta + 1$.

Before going to the pattern formation, here we discuss briefly the local asymptotic stability property of interior equilibrium point $E_*(n_*, p_*)$ for the temporal model corresponding to the spatio-temporal model (8.25). Calculating the quantities $j_{rs}, r, s = 1, 2$ we find,

$$j_{11} = \frac{\eta^2 \delta(1 - \delta) + 2\eta(1 - \delta) - 1}{(\delta \eta + 1)^2}, \ j_{12} = -\frac{1}{(\delta \eta + 1)^2}, \ j_{21} = \eta^2 \xi, \ j_{22} = -\eta \xi.$$

From these expression one can easily verify that the interior equilibrium point E_* is always locally asymptotically stable for $\delta \geq 1$ and we are unable to find any Turing pattern for the associated spatio-temporal model as $j_{11} j_{22} \geq 0$. For $\delta < 1$,
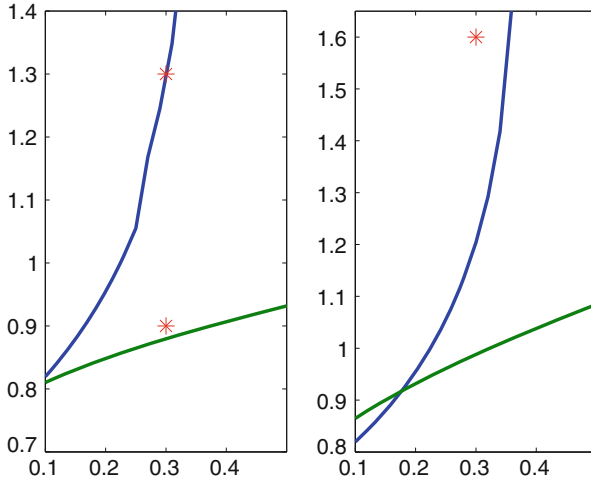
Fig. 8.6 Turing (*blue coloured*) and Hopf-bifurcation (*green coloured*) curves are drawn for $(\alpha, d) = (0.4, 25)$ (*left panel*) and $(\alpha, d) = (0.4, 10)$ (*right panel*) respectively. Hopf-bifurcation curve divides the Turing domain lying above the Turing domain into two regions. Parameter values for which numerical simulations are performed are marked with *red coloured stars*

E_* is locally asymptotically stable if $\xi > \left(\dfrac{\delta\eta + 2}{(\delta\eta + 1)^2} - \dfrac{1}{\eta} \right)$ and small amplitude periodic solution bifurcates from the coexisting equilibrium point through Hopf-bifurcation [8, 28]. Clearly, we will look at the Turing patterns for $\delta < 1$.

In the previous subsection, we have considered the ratio of diffusivity as bifurcation parameter and described various types of pattern formation by taking different values for d. Here we consider δ and d at some fixed values and consider η and ξ as bifurcation parameters. In other words, firstly we have to identify Turing and Turing-Hopf domain in the $\eta - \xi$ parameter space and then look at the various stationary and non-stationary patterns for the specific choices of parameter values. In Fig. 8.6 the Turing bifurcation curve and Hopf-bifurcation curve are plotted for $\alpha = 0.4$ and $d = 25$ and $d = 10$ respectively. Numerical simulations are performed for the parameter values within Turing domain and chosen parameter values are marked with red coloured stars in the bifurcation diagram. For the Holling-Tanner model with ratio-dependent functional response we find clod spot pattern and labyrinthine pattern for parameter values taken from Turing domain and Turing-Hopf domain respectively. These two patterns are obtained for $(\xi, \eta) = (0.3, 0.9)$ and $(\xi, \eta) = (0.3, 1.3)$ respectively and both the patterns presented in Fig. 8.7 are stationary patterns. Numerical simulations are performed with $\Delta t = 0.01, \Delta x = 1 = \Delta y$ and over 400×400 lattice and using zero flux boundary condition and small random perturbation around homogeneous steady-state as initial conditions.
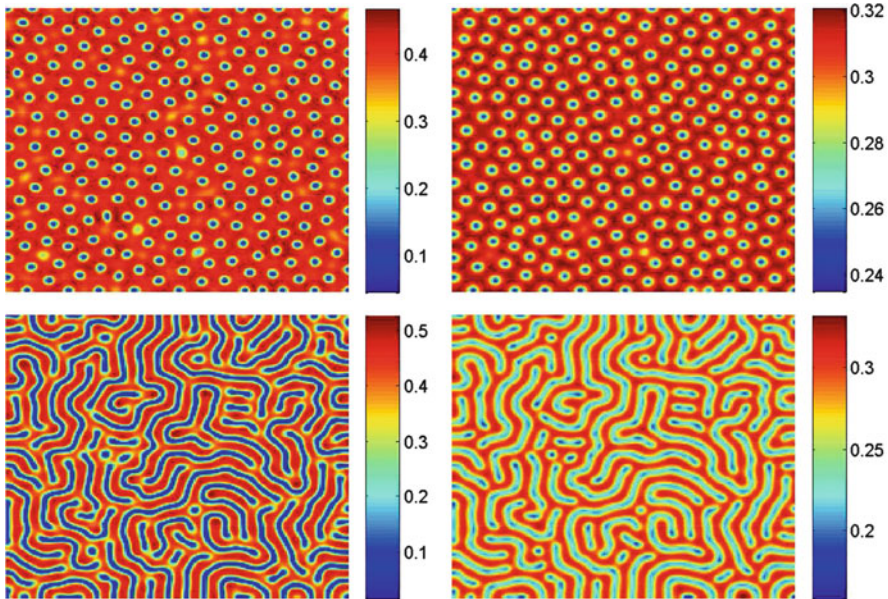
Fig. 8.7 Cold spot (*upper panel*) and labyrinthine pattern (*lower panel*) produced by prey (*left column*) and predator (*right column*) species, involved with the ratio-dependent Holling-Tanner model, at $t = 400$. Both of these patterns are obtained for fixed $\alpha = 0.4, \xi = 0.3, d = 25$ and $\eta = 0.9$ and $\eta = 1.3$ respectively

In the previous subsection we have considered the ratio of diffusivities as bifurcation parameter and illustrated how spatio-temporal chaos emerges for parameter values within and outside the Turing domain. Here it is important to note that the model under consideration in this subsection is unable to produce chaotic pattern when $d = 25$. Spatio-temporal chaotic pattern is obtained for the model (8.25) when $d \leq 12$, (for $\alpha = 0.4$) and some specific choices of ξ and η in the Turing-Hopf domain. Spatio-temporal chaotic pattern presented in Fig. 8.8 is obtained for $\alpha = 0.4, \xi = 0.3, \eta = 1.6$ and $d = 10$. This spatio-temporal chaos is a dynamic pattern as the distribution of prey and predators over two dimensional space changes continuously with the advancement of time. Patterns are checked for longer times also and it is observed that they never settle down to any stationary level. This model is also capable to produce interacting spiral type spatio-temporal chaotic pattern for $d = 1$ and not presented here to avoid repetitions.

8.3.3　Holling-Tanner Model

In the previous two subsections we have observed spatio-temporal patterns produced by prey-predator models with ratio-dependent functional response. Both the models
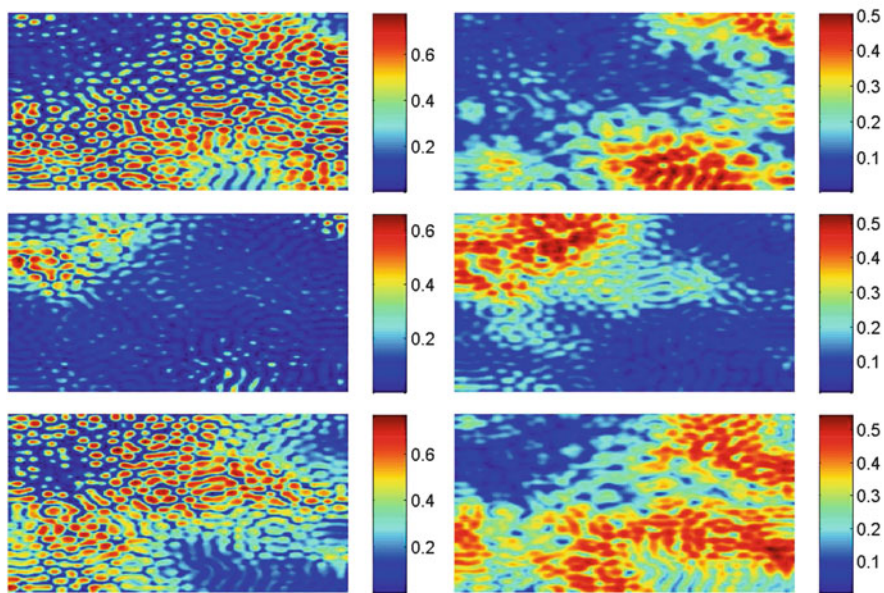
Fig. 8.8 Spatio-temporal chaotic pattern produced by prey (*left column*) and predator (*right column*) for the parameter values $\alpha = 0.4$, $\xi = 0.3$, $\eta = 1.6$ and $d = 10$. Patterns are obtained at $t = 1,000$ (*upper panel*); $t = 1,250$ (*lower panel*) and $t = 1,500$ (*lower panel*) respectively

produce cold spot and labyrinthine patterns as stationary patterns. Here we consider the spatio-temporal version of classical Holling-Tanner type prey-predator model to show the transition of Turing pattern from cold spot to hot spot through labyrinthine pattern and this transition takes place with gradual change in one parameter value. Turing and travelling wave patterns for this Holling-tanner model is recently investigated by Upadhyay et al. [65]. Spatio-temporal model for Holling-Tanner type prey-predator interaction is given by

$$\frac{\partial n(t, x, y)}{\partial t} = n(1 - n) - \frac{np}{n + v} + \left(\frac{\partial^2 n}{\partial x^2} + \frac{\partial^2 n}{\partial y^2} \right),$$

$$\frac{\partial p(t, x, y)}{\partial t} = \theta \left(1 - \frac{\xi p}{n} \right) p + d \left(\frac{\partial^2 p}{\partial x^2} + \frac{\partial^2 p}{\partial y^2} \right), \qquad (8.26)$$

subjected to the positive initial condition and no-flux boundary condition. Spatio-temporal pattern formation for this model is investigated in details by Upadhyay et al. [65] but the populations are labeled as phytoplankton and zooplankton respectively. The dynamical behavior of the temporal counterpart of the model (8.26) is well-known and available in the literature [43, 47, 62].

To show the transition if spatio-temporal pattern produced by the system (8.26), we consider the fixed parameter set $\nu = 0.1$, $\theta = 0.25$ and consider ζ as free parameter. For the chosen parameter set, we find the co-existing homogeneous steady-state $E_*(n_*, p_*)$ where

$$n_* = \zeta p_*, \quad p_* = \frac{9\zeta - 10 + \sqrt{121\zeta^2 - 180\zeta + 100}}{20\zeta^2}.$$

The condition for local asymptotic stability of co-existing equilibrium point for the associated temporal model can be obtained in terms of ζ. One important observation is that the equilibrium point loses its stability through Hopf-bifurcation at $\zeta_{H1} = 0.3227$ and regains its stability through another Hopf-bifurcation at $\zeta_{H2} = 1.0244$. Hopf-bifurcating limit cycle exist for $\zeta_{H1} \leq \zeta \leq \zeta_{H2}$.

The model (8.26) is simulated numerically keeping fixed the parameters $\nu = 0.1$, $\theta = 0.25$ and $d = 25$. Three different stationary patterns are obtained for $\zeta = 0.28$, $\zeta = 0.7$ and $\zeta = 1.15$. Numerical simulations are performed with the same set up as explained in the previous subsections. Three different Turing patterns are presented in Fig. 8.9.

For the chosen set of parameter values and considering ζ as parameter we find that the interior equilibrium point loses and regains the stability through two consecutive Hopf-bifurcations. The occurrence two successive Hopf-bifurcation
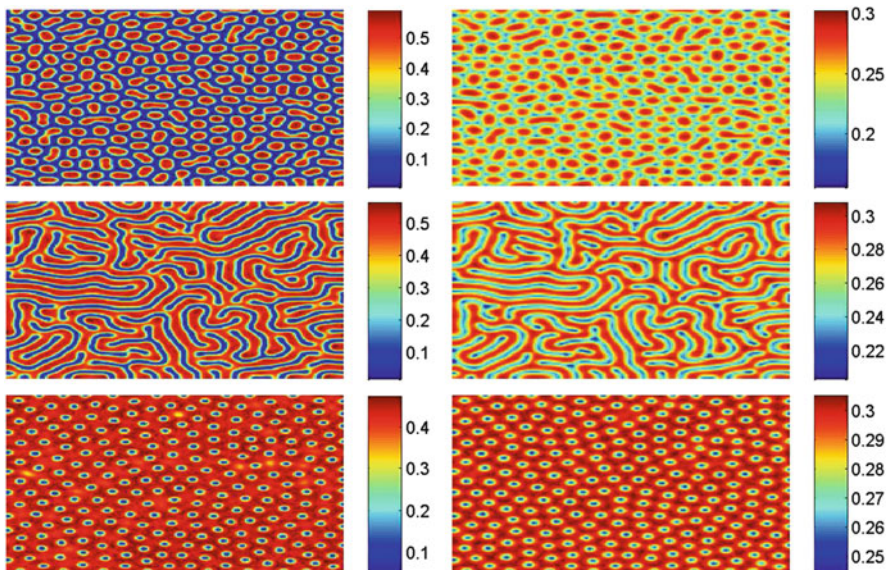

Fig. 8.9 Hot spot (*upper panel*; $\zeta = 0.28$), Labyrinthine (*middle panel*; $\zeta = 0.7$) and cold spot (*lower panel*; $\zeta = 1.15$) patterns are obtained through numerical simulation for varying ζ and keeping other parameters fixed at $\nu = 0.1$, $\theta = 0.25$ and $d = 25$. These stationary patterns are obtained at $t = 600$
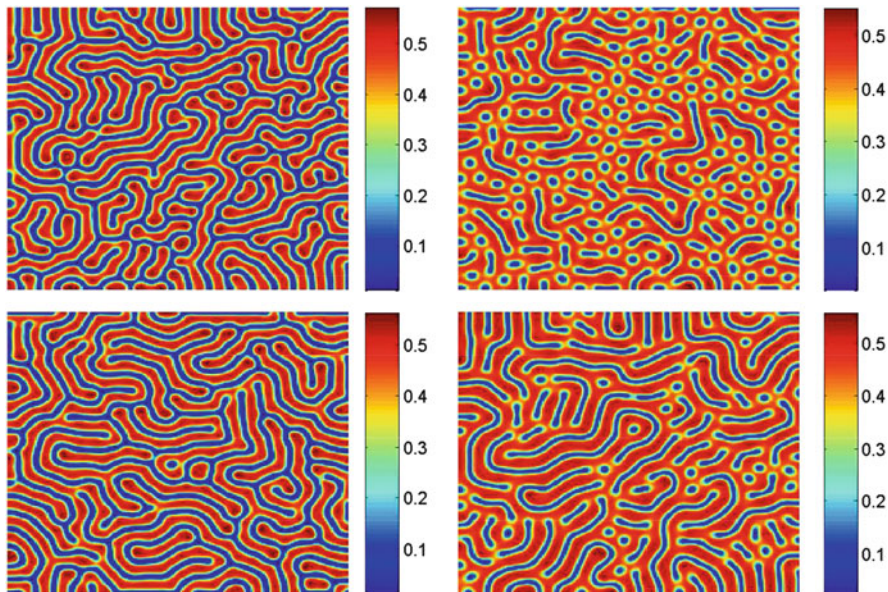
Fig. 8.10 Distribution of prey species over two dimensional landscape for $\zeta = 0.5$ (*left column*) and $\zeta = 0.9$ (*right column*) at $t = 500$, with $\nu = 0.1$, $\theta = 0.25$ and $d = 25$. Patterns presented in the *upper panel* are obtained with small random perturbation around homogeneous steady-state as initial condition and zero flux boundary condition. Patterns presented in the *lower panel* are obtained with the pattern obtained at $\zeta = 0.9$ and $\zeta = 0.5$ as initial conditions

is here responsible to generate hot spot and cold spot type Turing patterns. Labyrinthine pattern is observed for the parameter values lying in the Turing-Hopf domain. There is no spatio-temporal chaotic pattern exhibited by the model (8.26) for chosen set of parameter values.

An interesting phenomena for pattern formation takes place for this Holling-Tanner model when parameter values are inside the Turing-Hopf domain. Patterns produced by the prey and predator population are sensitive to initial conditions. Sensitivity of spatial pattern is presented in Fig 8.10. At the upper panel, patterns are obtained for two different values of the parameter ζ keeping other parameters fixed at the level as described above and with small random perturbation around the homogeneous steady-states as the initial conditions. The patterns are obtained for $\zeta = 0.5$ and $\zeta = 0.9$, they are stationary patterns. In order to check the sensitivity of initial condition, the stationary pattern obtained at $\zeta = 0.9$ is used as the initial condition and the spatio-temporal model is simulated numerically with $\zeta = 0.5$ and the stationary pattern obtained at $t = 500$ is presented at the left of lower panel in Fig. 8.10. Similarly, the pattern obtained for $\zeta = 0.5$ is used as initial condition to obtain the pattern when $\zeta = 0.9$ and we have obtained a different pattern compared to that was obtained with the usual initial condition used here.

8.4   Discussion

Autonomous temporal models of prey-predator interaction always results in either
stable stationary coexistence or oscillatory coexistence or extinction of one or both
the species. Spatio-temporal models are developed to take care of the mobility of
individuals over their habitats. Individuals of various species attempt to find out
most favorable habitat as well as patches where availability of their essential foods
is abundant. Again carnivorous predators have to chase their prey to get the food and
hence they have to run faster from their predators. Similarly, the swimming speed of
zooplankton within aquatic environment should be greater than the moving speed
of phytoplankton due to water current within the aquatic environment. All these
requirements are reflected through the condition $d > 1$, where d is the ratio of
diffusivities of the prey and their predators. At the initial stages of the research on
pattern formation, it was believed that the inequality in the ratio of diffusivity is
essential for spatio-temporal pattern formation. Afterwards, it is revealed that the
spatio-temporal patterns can emerge in case of equal diffusivities also [23, 41, 51].
Most important and interesting cases of pattern formation with equal diffusivities
are biological invasions and travelling wave-train [42, 45, 46, 58, 59, 61, 66, 67].
Recently, few authors have paid their attention towards the spatio-temporal chaotic
pattern formation due to wave of chaos. This scenario arises in most of the cases for
$d = 1$, (see [51, 64] and references cited therein).

In this chapter we have discussed pattern formation in prey-predator models
within Turing and Turing-Hopf domain with special emphasis on ratio-dependent
functional response. Prey-predator models with prey-dependent functional response
and intrinsic constant per capita death rate for predators are unable to produce
Turing patterns. Three models are considered here, ratio-dependent prey-predator
model, Holling-Tanner model with ratio-dependent functional response and classi-
cal Holling-Tanner model. The classical Holling-Tanner model is also known as
semi-ratio dependent model as the growth equation of the predators contains a
term which is proportional to the ratio of predator to prey. For fist two models,
we have observed that the stationary Turing patterns are cold spot patterns which
indicate the existence of circular patches with lower concentration of prey and
predators. In contrary, the stationary Turing patterns observed for the classical
Holling-Tanner model are of two types, hot spot pattern and cold spot pattern. Hot
spots are generated through the localized circular patches with high concentration of
population density. The labyrinthine pattern is observed for some particular choices
of parameter values within the Turing-Hopf domain. In the first two models, the
stationary cold spot pattern changed to labyrinthine pattern due to coalesce of nearby
circular patches with low concentration of population. This transition takes place as
parameter moves from Turing domain to Turing-Hopf domain. But the generation of
labyrinthine pattern in case of spatio-temporal Holling-Tanner model with Holling
type-II functional response can be explained in two ways. If we consider the increase
in the magnitude of ζ then labyrinthine pattern is generated by the coalescing of hot
spots and the same can be generated due the merging of nearby cold spots due

to decrease in the magnitude of ζ. The three models considered here are capable to generate another kind of stationary patterns which is a mixture of spot and labyrinthine pattern. The stationary patterns obtained for the first two models are independent of initial condition, we have checked this independence numerically but the results are not presented here. The sensitivity of resulting pattern, or in other words the dependence of stationary pattern on the choice of initial condition is illustrated for the spatially extended classical Holling-Tanner model. We have reported here the spatio-temporal chaotic patterns for parameter values within and outside the Turing domain. Obviously the spatio-temporal chaotic patterns are not stationary patterns rather they changes continuously with time and never settle down to any stationary state.

In reality the spot and labyrinthine patterns obtained within Turing domain are not realistic for the distribution of prey and predators distributed over two dimensional landscapes but can be observed for vegetation patterns generated through the interaction between autotroph and their herbivores. Again the patchy patterns resulting from spatio-temporal chaos and labyrinthine type distributions are observed for the vegetation patterns in semiarid regions [8, 14, 45, 69]. Spatio-temporal chaotic patterns are also observed for the distribution of various plankton biomass within aquatic environment. The discrepancy in the observed patterns are either due to the over simplification in the modeling approach or due to the consideration of distribution of individuals over two dimensional domain as a continuum media. The patterns obtained for the models under consideration give us the idea of size and rough shape of stationary patches for the distribution of prey and predator species. Some times they give indication of colony formation by the bacterial species and their predators. Apart from this distribution, the stationarity of patterns provide the information regarding the time invariant distribution of species over their spatial habitat.

Finally, we have addressed the issue of spatio-temporal chaotic patterns produced by prey-predator model with ratio-dependent functional response terms. Spatio-temporal chaotic pattern exists for parameter values within the Turing-Hopf domain as well as outside the Turing domain. Emergence of spatio-temporal chaos for parameter values above and below the Turing bifurcation curve ensures that the interaction between temporal instability and spatial instability is not essential for the onset of spatio-temporal chaos. Again, we have observed the existence of stationary patterns for the parameter values within Turing-Hopf domain, it means the coexistence steady-state of the reaction kinetics is unstable and local kinetics is oscillatory. These observations ensure the fact that the interaction between the temporal and spatial instability are unable to drive the system towards spatial and temporal irregularity under any circumstances. Rather the existence of irregular distribution of population over space and its continuous change with time depend upon the complex interaction is taking place over spatial and temporal scale. There are no unified criteria for the existence of spatio-temporal chaos. Further the mobility of individuals within their habitat has some role towards the patchy distribution of interacting populations. Recent works on continuous spatio-temporal models for interacting populations and vegetation distribution indicate the existence

of spatio-temporal chaos but the conclusive evidence in favor of chaotic patterns in realistic ecosystems are not abundant [20, 27, 46, 52, 54–56, 60]. Effect of cross-diffusion, periodic changes in essential resources, random environmental condition on the pattern formation for interacting population models with rich temporal dynamics needs appropriate attention to understand the complex dynamical behavior associated with the spatio-temporal pattern formation. Derivation of necessary and sufficient analytical conditions for the appearance of spatio-temporal chaotic patterns remain an open as well as challenging problem.

References

1. Akçakaya, H.R.: Population cycles of mammals: evidence for a ratio-dependent predator-prey hypothesis. Ecol. Monogr. **62**, 119–142 (1992)
2. Alonso, D., Bartumeus, F., Catalan, J.: Mutual interference between predators can give rise to turing spatial patterns. Ecology **83**, 28–34 (2002)
3. Arditi, R., Berryman, A.A.: The biological control paradox. Trends Ecol. Evol. **6**, 32–43 (1991)
4. Arditi, R., Ginzburg, L.R.: Coupling in predator-prey dynamics: ratio-dependence. J. Theor. Biol. **139**, 311–326 (1989)
5. Bandyopadhyay, M., Chattopadhyay, J.: Ratio-dependent predator-prey model: effect of environmental fluctuation and stability. Nonlinearity **18**, 913–936 (2005)
6. Banerjee, M.: Self-replication of spatial patterns in a ratio-dependent predator-prey model. Math. Comp. Model. **51**, 44–52 (2010)
7. Banerjee, M.: Spatial pattern formation in ratio-dependent model: higher-order stability analysis. IMA J. Math. Med. Biol. **28**, 111–128 (2011)
8. Banerjee, M., Banerjee, S.: Turing instabilities and spatio-temporal chaos in ratio-dependent Holling-Tanner model. Math. Biosci. **236**, 64–76 (2012)
9. Banerjee, M., Petrovskii, S.: Self-organized spatial patterns and chaos in a ratio-dependent predator-prey system. Theor. Ecol. **4**, 37–53 (2011)
10. Banerjee, M., Venturino, E.: A phytoplankton-toxic phytoplnkton-zooplankton model. Ecol. Complex. **8**, 239–248 (2011)
11. Baurmann, M., Ebenhoh, W., Feudel, U.: Turing instabilities and pattern formation in a Benthic nutrient-microorganism system. Math. Biosci. Eng. **1**, 111–130 (2004)
12. Baurmann, M., Gross, T., Feudel, U.: Instabilities in spatially extended predator-prey systems: spatio-temporal patterns in the neighborhood of Turing-Hopf bifurcations. J. Theor. Biol. **245**, 220–229 (2007)
13. Bazykin, A.D.: Nonlinear Dynamics of Interacting Populations. World Scientific, Singapore (1998)
14. Belsky, A.J.: Population and community processes in a mosaic grassland in the Serengeti, Tanzania. J. Ecol. **74**, 841–856 (1986)
15. Benson, D.L., Maini, P.K., Sherratt, J.: Pattern formation in reaction-diffusion models with spatially inhomogeneous diffusion coefficients. Math. Comp. Model. **17**, 29–34 (1993)
16. Benson, D.L., Sherratt, J., Maini, P.K.: Diffusion driven instability in an inhomogeneous domain. Bull. Math. Biol. **55**, 365–384 (1993)
17. Berezovaskaya, F.S., Karev, G., Arditi, R.: Parametric analysis of ratio-dependent predator-prey model. J. Math. Biol. **43**, 221–246 (2001)
18. Cantrell, R.S., Cosner, C.: Spatial Ecology Via Reaction-Diffusion Equations. Wiley, London (2003)
19. Cheng, K.S., Hsu, S.B., Lin, S.S.: Global stability of a predator-prey system. J. Math. Biol. **12**, 115–126 (1981)

20. Ellner, S., Turchin, P.: Chaos in a noisy world: new methods and evidence from time-series analysis. Am. Nat. **145**, 343–375 (1995)
21. Fasani, S. Rinaldi, S.: Factors promoting or inhibiting turing instability in spatially extended prey-predator systems. Ecol. Model. **222**, 3449–3452 (2011)
22. Freedman, H.I.: Deterministic Mathematical Models in Population Ecology. Marcel & Dekker, New York (1980)
23. Garvie, M.R.: Finite difference schemes for reaction-diffusion equations modeling predator-prey interactions in MATLAB. Bull. Math. Biol. **69**, 931–956 (2007)
24. Gause, G.F.: The Strugle for Existence. Williams and Wilkins, Baltimore (1935)
25. Gutierrez, A.P.: The physiological basis of ratio-dependent predator-prey theory: a metabolic pool model of Nicholson's blowflies as an example. Ecology **73**, 1552–1563 (1992)
26. Haldane, J.B.S.: Enzymes. Longman, London (1930)
27. Hanski, I., Turchin, P., Korplmakl, E., Henttonen, H.: Population oscillations of boreal rodents: regulation by mustelid predators leads to chaos. Nature **364**, 232–235 (1993)
28. Hassard, B.D., Kazarinoff, N.D., Wan, Y.H.: Theory and Application of Hopf-Bifurcation. Cambridge University Press, Cambridge (1981)
29. Hsu, S.B., Hwang, T.W., Kuang, Y.: Global analysis of the Michaelis–Menten type ratio-dependent predator-prey system. J. Math. Biol. **42**, 489–506 (2001)
30. Huisman, J., Weissing, F.J.: Biodiversity of plankton by oscillations and chaos. Nature **402**, 407–410 (1999)
31. Jost, C., Arino, O., Arditi, R.: About deterministic extinction in ratio-dependent predator-prey model. Bull. Math. Biol. **61**, 19–32 (1999)
32. Klausmeier, C.A.: Regular and irregular patterns in semiarid vegetation. Science **284**, 1826–1828 (1999)
33. Kot, M.: Elements of Mathematical Biology. Cambridge University Press, Cambridge (2001)
34. Kuang, Y.: Rich dynamics of Gause-type ratio-dependent predator prey system. Fields Inst. Commun. **21**, 325–337 (1999)
35. Kuang, Y., Beretta, E.: Global qualitative analysis of a ratio-dependent predator-prey system. J. Math. Biol. **36**, 389–406 (1999)
36. Kuznetsov, Y.A.: Elements of Applied Bifurcation Theory. Springer, New York (2004)
37. Levin, S.A., Segel, L.A.: Hypothesis for origin of planktonic patchiness. Nature **259**, 659 (1976)
38. Liang, Z., Pan, H.: Qualitative analysis of a ratio-dependent Holling-Tanner model. J. Math. Anal. Appl. **334**, 954–964 (2007)
39. Luckinbill, L.L.: Coexistence in laboratory populations of *Paramecium aurelia* and its predator *Didinium nasutum*. Ecology **54**, 1320–1327 (1973)
40. Luckinbill, L.L.: The effects of space and enrichment on a predator-prey system. Ecology **55**, 1142–1147 (1974)
41. Malchow, H.: Spatio-temporal pattern formation in nonlinear nonequilibrium plankton dynamics. Proc. R. Soc. Lond. B **251**, 103–109 (1993)
42. Malchow, H., Petrovskii, S.V., Venturino, E.: Spatiotemporal Patterns in Ecology and Epidemiology. Chapman & Hall, London (2008)
43. May, R.M.: Stability and Complexity in Model Ecosystems. Princeton University Press, New Jersey (2001)
44. Medvinsky, A., Petrovskii, S., Tikhonova, I., Malchow, H., Li, B.L.: Spatiotemporal complexity of plankton and fish dynamics. SIAM Rev. **44**, 311–370 (2002)
45. Morozov, A.Y., Petrovskii, S.V.: Excitable population dynamics, biological control failure, and spatiotemporal pattern formation in a model ecosystem. Bull. Math. Biol. **71**, 863–887 (2009)
46. Morozov, A.Y., Petrovskii, S.V., Li, B.L.: Bifurcation, chaos and intermittency in the predator-prey system with the Allee effect. Proc. R. Soc. Lond. B, **271**, 1407–1414 (2004)
47. Murray, J.D.: Mathematical Biology II. Springer, Heidelberg (2002)
48. Okubo, A., Levin, S.: Diffusion and Ecological Problems: Modern Perspectives. Springer, Berlin (2001)

49. Pal, R., Basu, D., Banerjee, M.: Modelling of phytoplankton allelopathy with Monod–Haldane-type functional response—a mathematical study. Biosystems **95**, 243–253 (2009)
50. Perko, L.: Differential Equations and Dynamical Systems. Springer, New York (2001)
51. Petrovskii, S.V., Malchow, H.: A minimal model of pattern formation in a prey-predator system. Math. Comp. Model. **29**, 49–63 (1999)
52. Petrovskii, S.V., Malchow, H.: Wave of chaos: new mechanism of pattern formation in spatio-temporal population dynamics. Theor. Popul. Biol. **59**, 157–174 (2001)
53. Petrovskii, S.V., Li, B.L., Malchow, H.: Quantification of the spatial aspect of chaotic dynamics in biological and chemical systems. Bull. Math. Biol. **65**, 425–446 (2003)
54. Petrovskii, S.V., Li, B.L., Malchow, H.: Transition to spatiotemporal chaos can resolve the paradox of enrichment. Ecol. Complex. **1**, 37–47 (2004)
55. Petrovskii, S., Morozov, A., Malchow, H., Sieber, M.: Noise can prevent onset of chaos in spatio-temporal population dynamics. Eur. Phys. J. B **78**, 253–264 (2010)
56. Scheffer, M.: Should we expect strange attractors behind plankton dynamics—and if so, should we bother? J. Plankt. Res. **13**, 1291–1305 (1991)
57. Segel, L.A., Jackson, J.L.: Dissipative structure: an explanation and an ecological example. J. Theor. Biol. **37**, 545–559 (1972)
58. Sherratt, J.A.: Periodic travelling waves in cyclic predator-prey systems. Ecol. Lett. **4**, 30–37 (2001)
59. Sherratt, J.A., Smith, M.: Periodic travelling waves in cyclic populations: field studies and reaction diffusion models. J. R. Soc. Interface **5**, 483–505 (2008)
60. Sherratt, J.A., Lewis, M.A., Fowler, A.C.: Ecological chaos in the wake of invasion. Proc. Natl. Acad. Sci. USA **92**, 2524–2528 (1995)
61. Shigesada, N., Kawasaki, K.: Biological Invasions: Theory and Practice. Oxford University Press, Oxford (1997)
62. Turchin, P.: Complex Population Dynamics. Princeton University Press, New Jersey (2003)
63. Turing, A.M.: The chemical basis of morphogenesis. Philos. Trans. R. Soc. Lond. B **237**, 37–72 (1952)
64. Upadhyay, R.K., Kumari, N., Rai, V.: Modeling spatiotemporal dynamics of vole populations in Europe and America. Math. Biosci. **223**, 47–57 (2010)
65. Upadhyay, R.K., Volpert, V., Thakur, N.K.: Propagation of Turing pattern in a plankton model. J. Biol. Dyn. **6**, 524–538 (2012)
66. Volpert, V., Petrovskii, S.V.: Reaction-diffusion waves in biology. Phys. Life Rev. **6**, 267–310 (2009)
67. Volpert, A., Volpert, V., Volpert, V.: Traveling Wave Solutions of Parabolic Systems. Translation of Mathematical Monographs, vol. 140. American Mathematical Society, Providence, RI (1994)
68. Wang, W., Liu, Q.X., Jin, Z.: Spatiotemporal complexity of a ratio-dependent predator-prey system. Phys. Rev. E **75**, 051913 (2007)
69. White, L.P.: Brousse tigrée patterns in southern Niger. J. Ecol. **58**, 549–553 (1970)
70. Xiao, D., Ruan, S.: Global dynamics of a ratio-dependent predator-prey system. J. Math. Biol. **43**, 268–290 (2001)